

## A STUDY OF THE GRAVITATIONAL WAVE FORM FROM PULSARS

S. R. VALLURI

*Department of Physics & Astronomy, University of Western Ontario, London, Ontario  
N6A 5B7, Canada  
Email: valluri@julian.uwo.ca*

F. A. CHISHTIE

*Department of Applied Mathematics, University of Western Ontario, London, Ontario  
N6A 5B7, Canada  
Email: fachisht@julian.uwo.ca*

R. G. BIGGS

*Department of Mathematics, University of Western Ontario, London, Ontario N6A 5B7,  
Canada  
Email: rbiggs@julian.uwo.ca*

M. DAVISON

*Department of Applied Mathematics, University of Western Ontario, London, Ontario  
N6A 5B7, Canada  
Email: mdavison@julian.uwo.ca*

SANJEEV V. DHURANDHAR

*Inter-University Centre for Astronomy and Astrophysics, Post Bag 4, Ganeshkhind ,  
Pune 411 007, India  
Email: sdh@iucaa.ernet.in*

B. S. SATHYAPRAKASH

*Department of Physics and Astronomy, University of Cardiff, Cardiff, UK  
Email: b.s.sathyaprakash@astro.cf.ac.uk*

We present analytical and numerical studies of the Fourier transform (FT) of the gravitational wave (GW) signal from a pulsar, taking into account the rotation of the Earth for a one day observation period.

### 1 INTRODUCTION

The direct detection of gravitational radiation (GR) from astrophysical sources is one of the most important outstanding problems in experimental gravitation today. The construction of large laser interferometric gravitational wave detectors like the LIGO<sup>1</sup>, VIRGO<sup>2</sup>, LISA, TAMA 300, GITO 6000 and AIGO is opening a new window for the study of a vast and rich variety of nonlinear curvature phenomena. The network of gravitational wave detectors can confirm that GW exist and by monitoring gravitational wave forms give important information on their amplitudes, frequencies and other important physical parameters.

A prototype of continuous astrophysical sources is a pulsar. A variety of instabilities cause deformations from spherical symmetry giving rise to GWs. The

amplitudes of GR from these pulsars are probably very weak ( $\leq 10^{-26} - 10^{-28}$ , for galactic pulsars). The GR signal will be buried deep within the noise of the detector system. The detection of a GR signal warrants the urgent need of careful data analysis with development of *analytical methods* and *problem oriented algorithms*.

In sections 2, 3 and 4 we outline the approach leading to the FT of the GW signal. The frequency modulation (FM), Doppler shift due to rotation and orbital motion of the Earth in the Solar System Barycentre (SSB) frame, its effect on the total phase of the received GW signal and the Fourier transform (FT) of the GW signal have previously been described<sup>2</sup>.

Sections 5 and 6 present discussion and conclusions.

## 2 Methodology

Typical values of the gravitational wave amplitude  $h$  for the Crab and Vela pulsars are  $\sim 10^{-25}$  and  $\sim 10^{-24}$  respectively. This amplitude is several orders of magnitude below LIGO's expected sensitivity of  $\sim 10^{-23}$ . Since the LIGO would make continuous observations over a time scale of a few months or more, a significant enhancement to the signal-to-noise ratio (SNR) is expected by integrating the data over a long time interval.

The total response of the detector is a function of the source position, the detector orientation, the orientation of the spin axis of the Earth and the orientation of the orbital plane. Since the pulsar signal is weak, long integration times  $\approx 10^7$  secs will be needed to extract the signal from the noise. Since the detector moves along with the Earth in this time, the frequency of the wave emitted by the source is Doppler shifted. Also since the detector has an anisotropic response, the signal recorded by the detector is both frequency and amplitude modulated. We discuss now the important role of frequency modulation in the context of signal detection.

## 3 Study of Frequency Modulated Pulsar Signal

Frequency modulation arises due to translatory motion of the detector acquired from the motion of the Earth. We consider only two motions of the Earth: its rotation about the spin axis and the orbital motion about the Sun, so the response is doubly frequency modulated with one period corresponding to a day and the other period corresponding to a year. The FM smears out a monochromatic signal into a small bandwidth around the signal frequency of the monochromatic waves. It also redistributes the power in a small bandwidth. The study of FM due to rotation of the Earth about its spin axis for a one day observation period shows that the Doppler spread in the angular bandwidth for 1kHz signal will be 0.029Hz. The Doppler spread in the angular bandwidth due to orbital motion for an observation period of one day will be  $1.7 \times 10^{-3}\text{Hz}^2$ .

Since any observation is likely to last longer than a day, *it is important to incorporate this effect in the data analysis algorithms*.

In order to study frequency modulation of a monochromatic plane wave, one must calculate the Doppler shift due to rotational and orbital motion of the Earth in the SSB frame. For this, we need to know relative velocity between the source

and detector. The Euler angles  $(\theta, \phi)$  give the direction of the incoming wave in the SSB frame. We characterize the motion of the Earth (and detector) simply: (a) We assume the orbit of the Earth to be circular. (b) We neglect the effect of the Moon on the motion of the Earth.

The phase  $\phi(t)$  of the Doppler shifted received signal for a single direction sky search  $(\theta, \phi)$  is given by,

$$\phi(t) = 2\pi \int_{t_0}^t f_{rec}(t') dt' \quad (1)$$

$$= 2\pi f_0 \int_{t_0}^t \left( 1 + \frac{\vec{v} \cdot \vec{n}}{c}(t') \right) dt' \quad (2)$$

$$= 2\pi f_0 \left[ t - t_0 + \left\{ \frac{A}{c} \sin \theta \cos \phi' + \frac{R}{c} \sin \alpha \{ \sin \theta (\sin \beta' \cos \varepsilon \sin \phi + \cos \phi \cos \beta') + \sin \beta' \sin \varepsilon \cos \theta \} \right\} - \left\{ \frac{A}{c} \sin \theta \cos \phi'_0 + \frac{R}{c} \sin \alpha \{ \sin \theta (\sin \beta'_0 \cos \varepsilon \sin \phi + \cos \phi \cos \beta'_0) + \sin \beta'_0 \sin \varepsilon \cos \theta \} \right\} \right]. \quad (3)$$

where  $\phi' = \omega_{orb}t - \phi$ ,  $\beta' = \beta_0 + \omega_{rot}t$ ,  $\phi'_0 = \omega_{orb}t_0 - \phi$ ,  $\beta'_0 = \beta_0 + \omega_{rot}t_0$ ,  $\beta_0$  is the initial azimuthal angle of the detector at the observation time  $t_0$ . where  $A$  is distance from the centre of the SSB frame to the centre of the Earth,  $R$  is the radius of the Earth, and  $\vec{n}$  the unit vector in the direction of source,  $\vec{n} = (\sin \theta \cos \phi, \sin \theta \sin \phi, \cos \theta)$ . Here we have assumed that at time  $t = 0$ , the longitudinal angle  $\beta = 0$ .

It can be seen from eq (3) that the Doppler corrections to the phase of received pulsar signal depends on the direction of the source in the sky. Orbital motion is omitted in this preliminary analysis but will be presented in later work.

#### 4 Fourier Transform Analysis of the FM signal due to the Rotational Motion of the Earth

We analyze the Fourier transform (FT) of the frequency modulated signal and study the extent to which the peak of the FT is smudged and to how much the FT *spreads* in the frequency space. This type of study would be useful from the point of view of data analysis and for applying such schemes as *stepping around the sky* method<sup>3</sup> which relies on the FT.

We let  $x = \frac{2\pi f_0 R}{c}$  and  $t_0 = 0$ . Here  $x$  plays the role of modulation index similar to  $K$  in the theory of signal modulation. The modulation index depends on the frequency of the pulsar signal. If we consider only the frequency modulated output of the signal, the output of amplitude unity is given as follows,

$$h(t) = \cos(\phi(t)). \quad (4)$$

We now consider the  $h(t)$  to be given on a finite time interval  $[0, T]$  which would be assumed to be the observation period. In our analysis we have assumed  $T$  to be

one day. The Fourier transform of the signal  $h(t)$  is given by,

$$\tilde{h}(f) = \int_0^T h(t) e^{-i2\pi ft} dt. \quad (5)$$

It is convenient to use a time coordinate  $\xi = \omega_{rot}t/2$  which for a period of a day is of the order of unity, *i.e* when  $T = 1\text{day} = 86400$  secs, the  $\xi_T = \omega_{rot}T = \pi$ .

An exact closed form expression for the Fourier transform of the frequency modulated GW signal is obtained by the analytical approach. The plane wave expansion in spherical harmonics is used. <sup>5</sup>

Then the GW signal becomes

$$\sum_{l,m} \int S_{lm}(f_0, \alpha, t) dt = \Re \int 4\pi \left[ \sum_{\rho=0}^{\infty} i^l Y_{lm}^*(\theta, \phi) e^{2\pi i f_0 t} j_l(k \sin(\omega_r t/2)) Y_{lm}(\alpha, \frac{\omega_r t}{2}) \right] dt \quad (6)$$

where  $\bar{K}$  is the wave vector with spherical coordinates  $(K, \theta, \phi)$  with

$$|K| = 4\pi f_0 \Re \sin \alpha (\sin(\omega_r t/2)) = k \sin(\omega_r t/2) \quad (7)$$

and  $\hat{n} = (n, \theta, \phi)$  ( $\hat{n} = 1$ ).

and the FT is given by

$$S_{lm}(f, f_0, \alpha) = FT(S_{lm}(f_0, \alpha, t)) \quad (8)$$

Further simplification gives:

$$\sum_{lm} S_{lm}(\omega, \omega_0, \alpha) = \sum_l \sum_m A_{lm} I(l, B, k) \quad (9)$$

where

$$A_{lm} = \frac{8}{\sqrt{2}} \pi^{3/2} i^l N_{lm} P_l^m(\cos \alpha) Y_{lm}^*(\theta, \phi) \quad (10)$$

and

$$N_{lm} = \sqrt{\frac{(2l+1)(l-|m|)!}{4\pi(l+|m|)!}} \quad (11)$$

With convenient co-ordinate transformations, we obtain

$$S_{lm}(\omega, \omega_0, \alpha) = A_{lm} I(l, B, k) \quad (12)$$

where

$$I(l, B, k) = \int_0^\pi \exp[iB\xi] \frac{J_{l+1/2}(k \sin \xi)}{\sqrt{k \sin \xi}} d\xi \quad (13)$$

Also,

$$I(l, B, k) = 2i^B \int_0^1 \frac{\cos(B \cos^{-1} x) J_{l+1/2}(kx)}{\sqrt{kx} \sqrt{1-x^2}} dx \quad (14)$$

(where  $B = 2(\frac{\omega_0 - \omega}{\omega_r}) + m$ )  
which equals

$$2\pi \frac{i^B k^{l+1/2}}{\sqrt{2} 2^{2l+1}} \frac{\Gamma(l+1)}{\Gamma(l+3/2)} \frac{{}_1F_3(l+1; l+3/2, (l+2+B)/2, (l+2-B)/2; -k^2/16)}{\Gamma((l+2+B)/2)\Gamma((l+2-B)/2)} \quad (15)$$

The  ${}_1F_3$  is the generalised hypergeometric function with one parameter (here  $l+1$ ) in the numerator and three parameters in the denominator and  $-k^2/16$  as its variable. A wealth of information is hidden in these parameters and  ${}_1F_3$  is uniformly convergent.

The numerical integration is done via the Clenshaw-Curtis quadrature algorithm and gives accurate and reliable results. Both the analytical and numerical results agree for  $k < 1$  and arbitrary  $l$ ; a result of possible relevance for LISA which observes the low frequency band 0.1 to 0.00001 Hz. For simultaneously large  $k$  and  $l$ , the factor  $k^{(l+1/2)}$  presents a challenge.

We also evaluate

$$|S_{lm}(K)|^2 \propto \frac{\pi k^{2l}}{4 2^{2l+1}} \frac{\Gamma(1/2)\Gamma(l+1/2){}_1F_2(l+1/2; 2l+2, l+3/2; -k^2)}{\Gamma(l+1)\Gamma(l+3/2)\Gamma(l+3/2)} \quad (16)$$

In this case we find perfect agreement with numerical results for  $k \leq 86$  and arbitrary  $l (\leq 300)$ . The above approach using the plane wave representation appears to be equally useful when orbital motion is also included in the analysis and will be discussed in future work involving orbital corrections.

## 5 Discussion

In general, the FT is a complex valued function of the parameters  $k$ ,  $l$  and  $B$ . Where appropriate, the absolute, real and the imaginary parts are taken. In Figure 1, the absolute value of the integral is plotted as a function of  $k$  for  $B = 30$  and  $l = 10$ . The maximum occurs around  $k = 40$ , which translates to approximately 150 Hz. The intensity drops off fast and is negligible around  $k = 300$ . Figure 2 again shows the absolute value of  $I$  vs  $k$  for  $B = 10$  but for  $l = 270 \gg 1$ . This plot shows remarkable evidence for the Bessel function index theorem as it shows  $I(k) = 0$  for  $k < 250$ , rising to a maximum around  $k = 285$  and falling off fast thereafter. For both large  $k$  and  $l$ ,  $B$  must be small to control the oscillations of the integrand to give a non-negligible value. Figure 3 shows absolute  $I$  vs  $B$  for  $l = k = 10$ . The integral peaks at  $B = 0$  and drops off fast around  $B = 6.25$  and rises again to a tiny value before dropping off to zero  $B \geq 10$ . Figure 4 shows absolute  $I$  vs  $B$  for  $l = k = 200 (\gg 1)$ . The integral peaks at  $B = 0$  then drops off rapidly at  $B > 20$ . This again illustrates that  $B$  has to be small to control the oscillations. Figure 5 shows absolute  $I$  vs  $B$  for  $l = 10$  and  $k = 270 (\gg 1)$ . Here the many bands of  $B$  are in full display until  $B \leq 280$ . Figure 6 shows the absolute value  $|S_{lm}(k)|^2$  vs  $l$  and  $k$  for the indicated range.

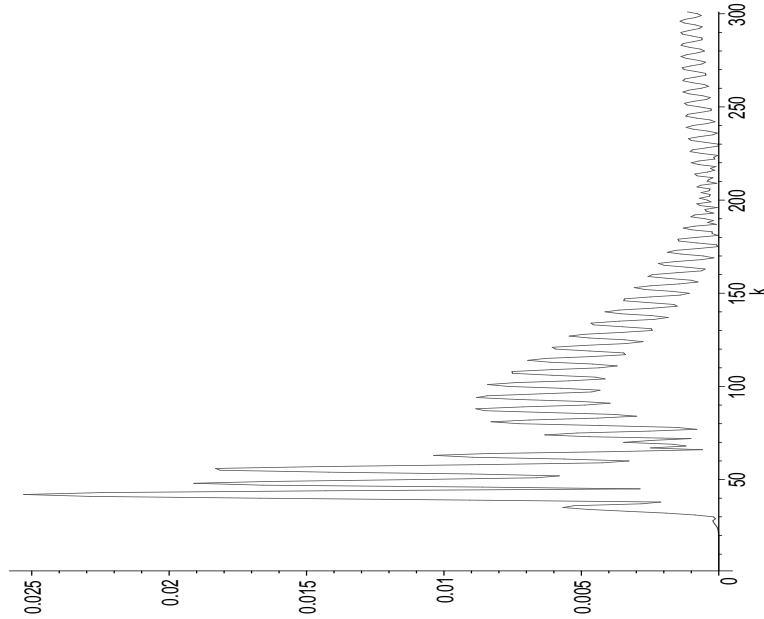


Figure 1.  $|I(l, k, B)|$  vs  $k$  for  $B = 30, l = 10$

## 6 Conclusion

We have studied the frequency modulation of the pulsar signal by two different methods. A closed form of the Fourier transform of the frequency modulated GW pulsar signal due to rotational motion of the Earth about its spin axis has been obtained. The work with the inclusion of orbital corrections results in a double series with only a finite number of surviving terms. Further details of this analysis warrant study and will be presented in later work<sup>6</sup>. Deeper results would be useful for schemes like the stepping around the sky method<sup>3</sup> and for differential geometric methods that allow the setup of search templates in the relevant parameter space<sup>4</sup>. This analysis should also be applicable to the Doppler modulation of the GW signal caused by LISA's orbit around the sun.

## References

1. A. Abramovici et al, *Science*, **256**, 325 (1992).
2. K. Jotania, S. Valluri, and S.V. Dhurandhar, *Astron & Astrophys* **306**, 317 (1996).
3. B.F. Schutz, in *The Detection of Gravitational Waves*, ed. D.G. Blair (Cambridge University Press,1991).
4. B.S. Sathyaprakash, Filtering gravitational waves from Supermassive Black Hole Binaries, *LISA Conference, CALTECH*(1998).
5. B.H. Bransden & C. J. Joachain, *Intoduction to Quantum Mechanics*, John

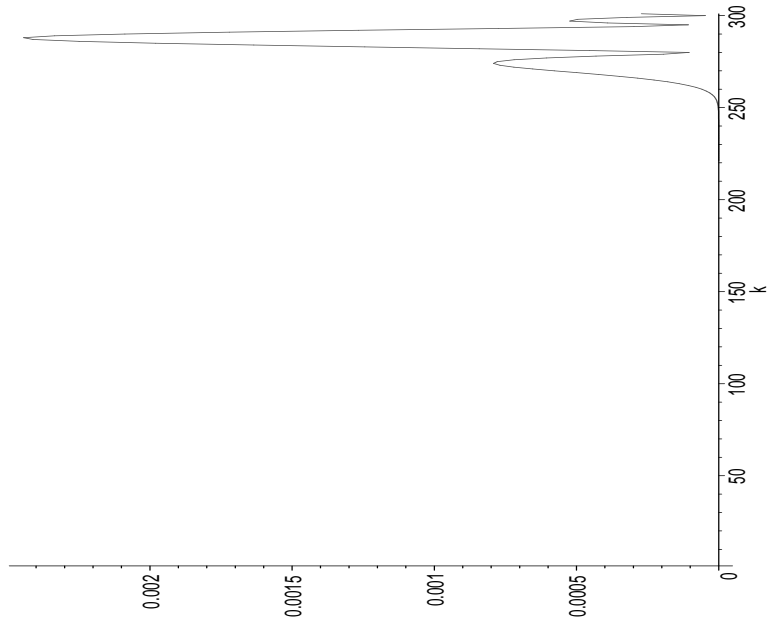
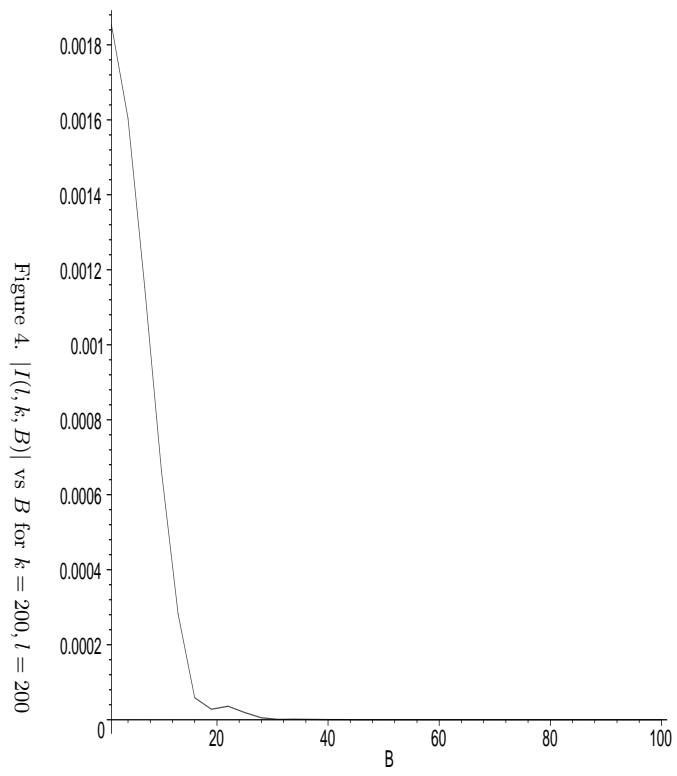
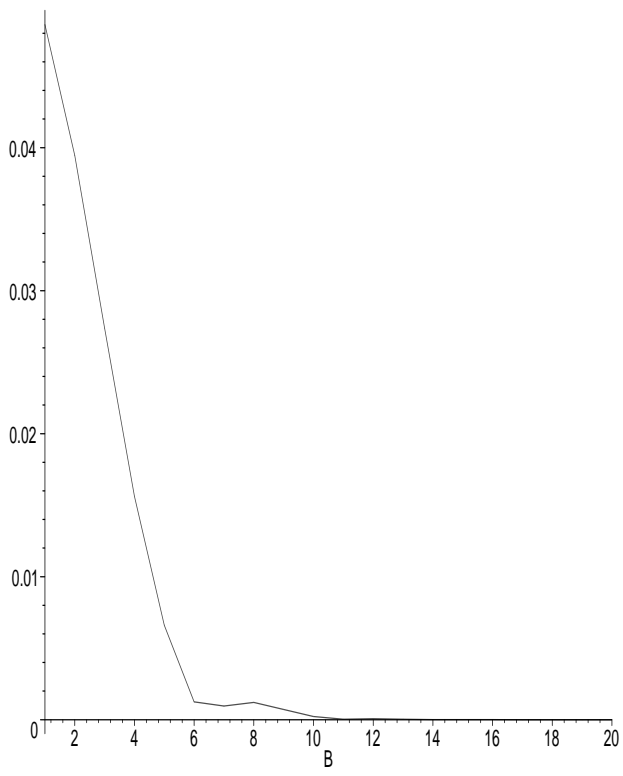


Figure 2.  $|I(l, k, B)|$  vs  $k$  for  $B = 10, l = 270$ , width=10cm, height=9cm

Wiley 2000.

6. S.R. Valluri et al, 2000, (in preparation).





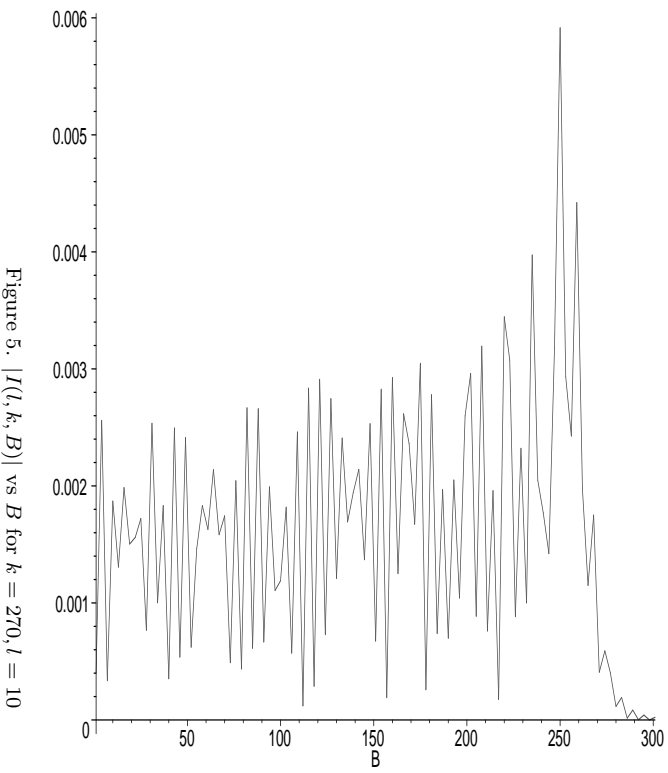


Figure 5.  $|I(l, k, B)|$  vs  $B$  for  $k = 270, l = 10$

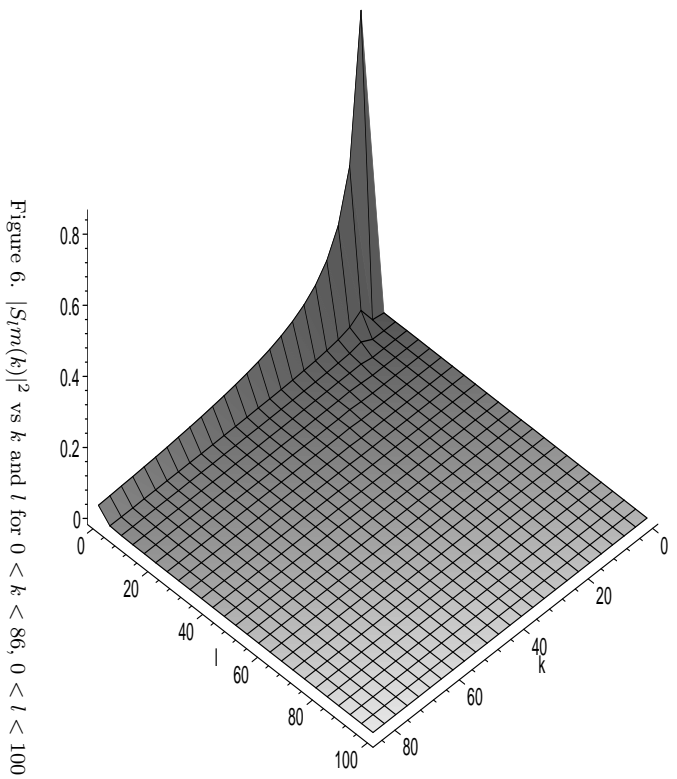


Figure 6.  $|S_l m(k)|^2$  vs  $k$  and  $l$  for  $0 < k < 86, 0 < l < 100$